Canadian Journal of
Forest Research

Article

Increased leaf area compensated photosynthetic downregulation in response to elevated CO_2 and warming in white birch

Lei Wang[a,b], **Jinping Zheng**[a,c], **Gerong Wang**[a,c], **and Qing-Lai Dang**[a]

[a]Faculty of Natural Resources Management, Lakehead University, 955 Oliver Road, Thunder Bay, ON P7B 5E1, Canada; [b]Department of Biotechnology, College of Biotechnology, Jiangsu University of Science and Technology, Zhenjiang, Jiangsu 212003, China; [c]Forestry College, Beihua University, 3999 Binjiang East Road, Jilin, Jilin 132013, China

Corresponding author: **Qing-Lai Dang** (email: qdang@lakeheadu.ca)

Abstract

Predicting photosynthetic acclimation to elevated CO_2 and warming is difficult because they have opposite effects. We investigated physiological and morphological responses in white birch (*Betula papyrifera* Marshall) to a combination of CO_2 and temperature (ACT — 400 μmol·mol^{-1} CO_2, current temperature; ECT — 750 μmol·mol^{-1} CO_2, current + 4 °C temperature). ECT reduced photosynthesis, maximum Rubisco carboxylation (V_{cmax}), maximum electron transport rate (J_{max}), photorespiration, daytime respiration, leaf N, and stomatal and mesophyll conductance, but increased biomass, height, total leaf area, electron partitioning to carboxylation and oxygenation ratio, and CO_2 compensation point. The photosynthetic acclimation is consistent with the optimal carbon gain theory (carbon gain drives the coordination of carboxylation, electron transport, and respiration). While the photosynthetic acclimation was similar to acclimation to elevated CO_2, ECT reduced J_{max}/V_{cmax}, which is consistent with the response to warming but opposite to the response to elevated CO_2, suggesting that thermal acclimation may be the primary mechanism of photosynthetic acclimation to ECT and ECT probably altered N allocation between machinery for carboxylation and that for ribulose-1,5-bisphosphate regeneration. The increase in total leaf area by ECT more than offset the negative effect of photosynthetic downregulation on carbon sequestration, resulting in faster growth and greater biomass under ECT.

Key words: white birch (*Betula papyrifera* Marshall), elevated CO_2, photosynthetic acclimation, electron transport, leaf area, carbon gain

Résumé

Il est difficile de prédire l'acclimatation photosynthétique à un taux élevé de CO_2 et au réchauffement, car ils ont des effets opposés. Nous avons étudié les réponses physiologiques et morphologiques du bouleau gris (*Betula papyrifera* Marshall) à une combinaison de CO_2 et de température (ACT : 400 μmol·mol^{-1} CO_2, température actuelle ; ECT : 750 μmol·mol^{-1} CO_2, température actuelle + 4 °C). L'ECT a réduit la photosynthèse, la carboxylation maximale de la Rubisco (V_{cmax}), la vitesse maximale de transport des électrons (J_{max}), la photorespiration, la respiration diurne, l'azote foliaire, la conductance stomatique et mésophylle, mais a augmenté la biomasse, la hauteur, la surface foliaire totale, le ratio de partage des électrons vers la carboxylation et l'oxygénation et le point de compensation du CO_2. L'acclimatation photosynthétique est conforme à la théorie du gain optimal de carbone (le gain de carbone détermine la coordination de la carboxylation, du transport d'électrons et de la respiration). Alors que l'acclimatation photosynthétique était similaire à l'acclimatation au CO_2 élevé, l'ECT a réduit J_{max}/V_{cmax}, ce qui est cohérent avec la réponse au réchauffement mais opposé à la réponse au CO_2 élevé, suggérant que l'acclimatation thermique peut être le mécanisme principal de l'acclimatation photosynthétique à l'ECT et que l'ECT a probablement modifié l'allocation de l'azote entre la machinerie pour la carboxylation et celle pour la régénération du RuBP (« ribulose-1,5-bisphosphate »). L'augmentation de la surface foliaire totale par l'ECT a plus que compensé l'effet négatif de la dérégulation photosynthétique sur la séquestration du carbone, ce qui a entraîné une croissance plus rapide et une plus grande biomasse sous l'ECT. [Traduit par la Rédaction]

Mots-clés : bouleau gris (*Betula papyrifera* Marshall), CO_2 élevé, acclimatation photosynthétique, transport d'électrons, surface foliaire, gain de carbone

Introduction

Atmospheric CO_2 is expected to continue to increase in the foreseeable future, along with increasing temperature (Kurepin et al. 2018). The associated climate change will have far-reaching impacts on vegetation (Tcherkez et al. 2017). Climate change may increase the probability of extreme weather events, posing serious challenges to both natural vegetation and cultivated crops (Birami et al. 2020; Slot et al. 2021). Long-term elevated CO_2 reduces photosynthetic capacity and leaf nitrogen (N) concentration (Dusenge et al. 2019; Dingkuhn et al. 2020) but promotes plant growth by 10%–30% (Kimball 2016; Pastore et al. 2019). A good understanding of the mechanisms of plant morphological and physiological responses to elevated CO_2 and temperature is the basis for predicting the impacts of climate change and for developing adaptive strategies (Tcherkez et al. 2017).

The effects of single factors such as increasing CO_2 or temperature on plant growth have been well studied. It is believed that elevated CO_2 induces photosynthetic acclimation of plants (Smith and Keenan 2020), which is manifested by reducing photosynthetic capacity (V_{cmax}, J_{max}), and nitrogen content, and inhibiting the respiration of leaves (Birami et al. 2020; Dusenge et al. 2020; Ainsworth and Long 2021) (Table 1). Warming can cause thermal acclimation of plants (Murphy and Way 2021). For example, an appropriate temperature rise can increase the activation energy of carboxylation and oxidation rubisco, reduce J_{max}/V_{cmax}, accelerate photosynthesis-related biochemical processes, and drive carbon sink intensity (Smith and Dukes 2017; Weigt et al. 2018). However, there was no relatively unified conclusion on the combined effect of elevated CO_2 and temperature on plants. Some studies found positive interaction between elevated temperature and CO_2 (Ainsworth and Long 2021), which promoted growth and increased resistance of plants (Apgaua et al. 2019). Other research suggests that the two factors have no obvious interaction or that their effects offset each other (Dusenge et al. 2019, 2020). Therefore, it is difficult to predict the combined effect of elevated temperature and CO_2 (Jayawardena et al. 2019).

Photosynthetic acclimation is a typical manifestation of plant long-term growth under elevated CO_2 and has been found to be independent of growth temperature and water conditions (Salazar-Parra et al. 2015). Photosynthetic acclimation usually resulted in a significant decrease in leaf V_{cmax} and J_{max} (Murphy and Way 2021); however, it stimulates an increase in plant biomass (Apgaua et al. 2019). These processes are also profoundly affected by temperature changes (Bermudez et al. 2021). Considering that elevated atmospheric CO_2 drives global warming, the effects of elevated temperature and CO_2 on plants are shown indistinguishable under future climate change conditions (Ainsworth and Long 2021). Therefore, it is important to investigate the characteristics of photosynthesis by combining elevated temperature and CO_2 treatments.

White birch (*Betula papyrifera* Marshall) is a widely distributed tree species in the Changbai Mountain forest region in China. It has great ecological values to the ecosystem as well as one of the most valuable commercial species in the region. This study evaluated the photosynthetic and morphological responses of the species to the elevations of CO_2 and temperature to elucidate the physiological mechanisms of the responses. We discussed the coordination between physiological and morphological parameters in the context of whole tree response. Further, we attempted to synthesize the response mechanisms of trees based on our findings and the literature.

Materials and methods

Plant materials

White birch (*B. papyrifera*) seeds were collected from a natural forest in the Changbai Mountain (42°12′N, 127°51′E) of China in 2018. Seeds were germinated in germination trays (50 cm × 25 cm × 5 cm) filled with a mixture of vermiculite and peat moss (1:1, *v*:*v*) in the Lakehead University greenhouse complex (Thunder Bay). The temperatures and photoperiod during the germination were set to 25/16 °C (day/night) and 16 h. Natural light was supplemented with high-pressure sodium lamps when the flux density of photosynthetically active radiation (PAR) was below 500 $\mu mol \cdot m^{-2} \cdot s^{-1}$. The seedlings were transplanted into 3.5 L pots with the same growing medium as used in the germination when they developed two leaves.

Experimental design and treatments

The experiment was conducted in four environment-controlled greenhouses at Lakehead University (Thunder Bay). The combined treatment of CO_2 and temperature (CT) had two levels (Table 1): (*i*) ACT = ambient CO_2 (400 $\mu mol \cdot mol^{-1}$) and current temperature (25/16 °C day/night temperatures); (*ii*) ECT = elevated CO_2 (750 $\mu mol \cdot mol^{-1}$) and elevated temperature (current + 4 °C, 29/20 °C day/night temperature). The experimental design was randomized block. Each treatment level had two independent replicates (total of four separate greenhouses) and the replicates green house as blocking factor. Since there may be a position effect within the same greenhouse (Potvin and Tardif 1988), the positions of trees within the same greenhouse were rotated weekly. There were six seedlings in each treatment–replicate combination. All the seedlings were irrigated to the drip point every 2 days and fertilized twice a week with a fertilizer solution containing 150 $mg \cdot L^{-1}$ nitrogen using All-purpose 25–10–25 N–P–K fertilizer (Plant Products Co. Ltd.).

The environmental conditions of the greenhouses (i.e., temperature, light, photoperiod, CO_2, and humidity) were monitored and controlled with an Argus Titan Environment-control system (Argus Control Systems Ltd., Vancouver, BC, Canada). The CO_2 elevation was achieved using CO_2 generators (model GEN-2E; Custom Automated Products Inc., Riverside, CA, USA) which were controlled by the Argus system.

Measurements of biomass, height growth, and foliar N

Seedling height was measured at the end of the experiment. The total leaf area per tree was measured using Regent

Table 1. Definition of acronyms.

Acronym	Definition	Unit
A/C_i	Net photosynthesis rate vs. intercellular CO_2 concentration response curve	—
ACE	Apparent carboxylation efficiency	—
ACT	Treatment of ambient 400 μmol·mol^{-1} CO_2 and ambient temperature	—
A_n	Net photosynthesis rate	μmol·m^{-2}·s^{-1}
A_{n-t}	A_n at the transition point from RuBP carboxylation to regeneration limitation	μmol·m^{-2}·s^{-1}
ACT-C400	ACT treated seedlings gas exchange measured at 400 μmol·mol^{-1} CO_2	—
ACT-C750	ACT treated seedlings gas exchange measured at 750 μmol·mol^{-1} CO_2	—
C400	400 μmol·mol^{-1} of CO_2 concentration	μmol·mol^{-1}
C750	750 μmol·mol^{-1} of CO_2 concentration	μmol·mol^{-1}
CCP_{aci}	CO_2 compensation point from A/C_i curve	μmol·mol^{-1}
C_i*	Intercellular CO_2 compensation point	μmol·mol^{-1}
C_{i-t}	C_i at the transition point between RuBP carboxylation to regeneration limitation	μmol·mol^{-1}
C_i/C_a	Intercellular (C_i) to ambient (C_a) CO_2 concentration ratio	—
ECT	Treatment of 750 μmol·mol^{-1} CO_2 and elevated temperature (ambient + 4 °C)	—
ECT-C400	ECT treated seedlings' gas exchange was measured at 400 μmol·mol^{-1} CO_2	—
ECT-C750	ECT treated seedlings' gas exchange was measured at 750 μmol·mol^{-1} CO_2	—
ΦPHII	Photochemical efficiency of photosystem II	—
g_s	Stomatal conductance	mmol·m^{-2}·s^{-1}
g_m	Mesophyll conductance	mol·m^{-2}·s^{-1}
iWUE	Instantaneous photosynthetic water use efficiency	mmol·m^{-2}·s^{-1}
J_c	Electron transport to carboxylation	μmol·m^{-2}·s^{-1}
J_o	Electron transport to oxygenation	μmol·m^{-2}·s^{-1}
J_{max}	Maximum photosynthetic electron transport rate	μmol·m^{-2}·s^{-1}
LMR	Leaf mass ratio	—
N_{area}	Leaf N content based on leaf-area	g·m^{-2}
N_{mass}	Leaf N concentration-based mass	mg·g^{-1}
R_d	Daytime respiration	μmol·m^{-2} s^{-1}
SLA	Specific leaf area	g·m^{-2}
SMR	Stem mass ratio	—
V_{cmax}	Maximum rate of RuBP carboxylation	μmol·m^{-2}·s^{-1}

WinFolia (Regent Instruments Inc., Québec, QC, Canada). All the plant organs were oven-dried at 80 °C for 48 h to obtain biomasses, root–shoot ratio, leaf mass ratio (LMR), stem mass ratio (SMR), root mass ratio (RMR), and specific leaf area (SLA). Leaf N concentration (all fully expanded leaves) was assayed by the Lakehead University Centre for Analytical Services using the dry combustion method with a CNS-2000 (LECO Corp., St. Joseph, MI, USA). The mass-based leaf N concentration (N_{mass}, mg·g^{-1}) was converted to area-based leaf N concentration (N_{area}, g·m^{-2}) using the SLA.

A/C_i curves and calculations of V_{cmax} and J_{max}

Three seedlings were randomly selected from each replicate–treatment combination after 2 months of treatment. The gas exchange was measured on the first fully expanded leaf from the top using a PP-Systems CIRAS-3 Portable Photosynthesis System equipped with a PLC3 Universal Leaf Cuvette with automatic climate control and a built-in CFM-3 Chlorophyll Fluorescence Module (PP Systems International, Inc., Amesbury, MA, USA). Photosynthetic response to CO_2 (A/C_i) curves were measured at 400, 300, 200, 150, 100, 50, 400, 500, 750, 900, 1100, and 1300 μmol·mol^{-1} CO_2 (C_a), 25 °C leaf temperature, 800 μmol·m^{-2}·s^{-1} PAR and 50% RH. The A/C_i data were analyzed using the Plantecophys fitaci function of the R package to produce the maximum carboxylation rate of ribulose-1,5-bisphosphate (RuBP) (V_{cmax}, μmol·m^{-2}·s^{-1}), and the maximum electron transport rate of photosynthesis (J_{max}, μmol·m^{-2}·s^{-1}) (Duursma 2015). The slope of initial light response curve was performed at 400 μmol·mol^{-1} CO_2 and 50, 100, 150, 200, 300 μmol·m^{-2}·s^{-1} PAR to obtain the quantum yield (ΦPHII).

G_m, J_c, J_o, R_l, and R_t estimates

Laisk script measurements (Walker and Cousins 2013) were taken at 200, 150, 100, and 50 μmol·mol^{-1} CO_2 concentration and 300, 150, and 75 μmol·m^{-2}·s^{-1} PAR to estimate the daytime respiration (R_d) and intercellular CO_2 compensation point (C_i*) (Farquhar et al. 1980). The variable J method was used to estimate the mesophyll conductance, g_m (Harley et al. 1992), where the electron transport (J) was calculated from chlorophyll fluorescence measurement according to

Momayyezi's protocol and $\Gamma*$ was assumed to be equal to C_i* (Momayyezi and Guy 2017). The chlorophyll fluorescence measurement was taken using the built-in CFM-3 model in the PP Systems CIRAS-3 system.

From the combination of chlorophyll fluorescence data (J), A_n and R_d estimated using the Laisk method, J_c (electron transport to carboxylation), J_o (electron transport to oxygenation), R_l (photorespiration rate), and R_t (leaf total respiration under light) were obtained as follows (Valentini et al. 1995; Tomeo and Rosenthal 2018):

$$(1) \quad J_c = [J + 8(A_n + R_d)]/3$$

$$(2) \quad J_o = [J - 4(A_n + R_d)]2/3$$

$$(3) \quad R_l = [J - 4(A_n + R_d)]/12$$

Gas exchange measurements at 400 and 750 CO_2

To assess treatment effects on the actual photosynthetic performance, the gas exchange of trees in both CO_2 treatments were measured at both growth CO_2 concentrations, i.e., at 400 and 750 μmol·mol^{-1} C_a. The following parameters from these measurements were assessed: net photosynthetic rate (A_n), the ratio of intercellular to ambient CO_2 (C_i/C_a), stomatal conductance (g_s), transpiration rate (E), and instantaneous water use efficiency (iWUE). The responses to the measured C_a and interactions with treatment (ACT vs. ECT) were tested using a two-way ANOVA.

Statistical analyses

The effects of CO_2–temperature treatments were tested using the Student's t test. The data were examined for the normality of distribution (using probability plots for residuals) and the homogeneity of variance (using scatter plots). Regression analyses were conducted on the relationships between leaf area, A_{n-t} and relevant physiological variables. Principal component analysis (PCA) was applied to all the physiological and biomass parameters using the PCA function from the FactoMineR package. Pearson correlation analyses were performed to examine the relationships of CCP_{aci} and J_c/J_o to the photosynthetic and growth variables. Effects of measurement CO_2 (400 vs. 750 μmol·mol^{-1}) and CT treatments (ACT vs. ECT) were tested using two-way ANOVA. All the analyses were performed using the R Package 4.0.4.

Table 2. P values of Student's t test for the effects of [CO_2]–temperature treatment (ACT: ambient CO_2 (400 μmol·mol^{-1}) and ambient temperature vs. ECT: elevated CO_2 (750 μmol·mol^{-1}) and elevated temperature (ambient + 4 °C)) on biomass, growth, and photosynthetic variables of white birch seedlings.

Variable	P value
Biomass	**0.002**
RMR	**0.034**
SMR	**<0.001**
LMR	0.308
Root–shoot ratio	**0.04**
Leaf area	**0.015**
Hight	**<0.001**
SLA	0.769
N_{area}	**0.006**
N_{mass}	**0.002**
J_{max}/N_{area}	**0.012**
R_d	**<0.001**
C_i*	**0.033**
V_{cmax}	**<0.001**
J_{max}	**<0.001**
J_{max}/V_{cmax}	**<0.001**
C_{i-t}	0.187
A_{n-t}	**<0.001**
CCP_{aci}	**<0.001**
ACE	**<0.001**
R_l	**<0.001**
ΦPHII	**<0.001**
J_c	**<0.001**
J_o	**<0.001**
J_c/J_o	**0.004**
g_m	**<0.001**

Note: Significant effects ($P \leq 0.05$) are in bold. RMR, root mass ratio; SMR, stem mass ratio; LMR, leaf mass ratio; SLA, specific leaf area; N_{area}, leaf N content based on leaf area; N_{mass}, leaf N concentration based mess; J_{max}/N_{area}, maximum electron transport rate based leaf N; R_d, daytime respiration; C_i*, intercellular CO_2 compensation point; V_{cmax}, maximum rate of ribulose-1,5-bisphosphate carboxylation; J_{max}, maximum of photosynthetic electron transport rate; J_{max}/V_{cmax}, the ratio of J_{max} to V_{cmax}; C_{i-t}, intercellular CO_2 at the transition point between rubisco limitation and RuBP regeneration limitation based on A/C_i curve; A_{n-t}, net photosynthesis rate at C_{i-t}; CCP_{aci}, CO_2 compensation point from A/C_i curve; ACE, apparent carboxylation efficiency; R_l, photorespiration rate; ΦPHII, photochemical efficiency of photosystem II; J_c, electron transport to carboxylation; J_o, electron transport to oxygenation; J_c/J_o, ratio of J_c to J_o; g_m, mesophyll conductance.

Results

Biomass, growth, and photosynthesis

ECT significantly increased biomass, height, leaf area, and SMR (Table 2; Figs. 1A–1C, 1E), but decreased root–shoot ratio, RMR, and foliar N concentration (Table 2; Figs. 1D, 1F–1H). The ECT also significantly reduced most of the photosynthetic parameters (Tables 2 and 3) but increased C_i* and J_c/J_o (Table 3).

The PCA results corroborated well with the Student's t test findings (Fig. 2). The seedlings exposed to ECT clustered in the left direction with growth parameters, CCP_{aci}, C_i*, and J_c/J_o, while the seedlings in ACE tended to cluster in the right direction with photosynthetic and leaf N concentration parameters (Fig. 2). The PCA results show that CCP_{aci} and J_c/J_o were negatively correlated with photosynthetic pa-

Fig. 1. Effects of CO_2–temperature treatment on total seedling biomass (A), height (B), total leaf area (C), root–shoot ratio (D), stem mass ratio (SMR) (E), root mass ratio (RMR) (F), leaf-area based N concentration (G), and leaf-mass based N concentration (H) in white birch seedlings. The seedlings were grown either under ACT (ambient 400 μmol·mol^{-1} CO_2 and ambient temperature) or ECT (750 μmol·mol^{-1} CO_2 and elevated temperature (ambient + 4 °C)). Means (±1.96 × SE, $n = 6$) with different letters were significantly different from each other ($P \leq 0.05$).

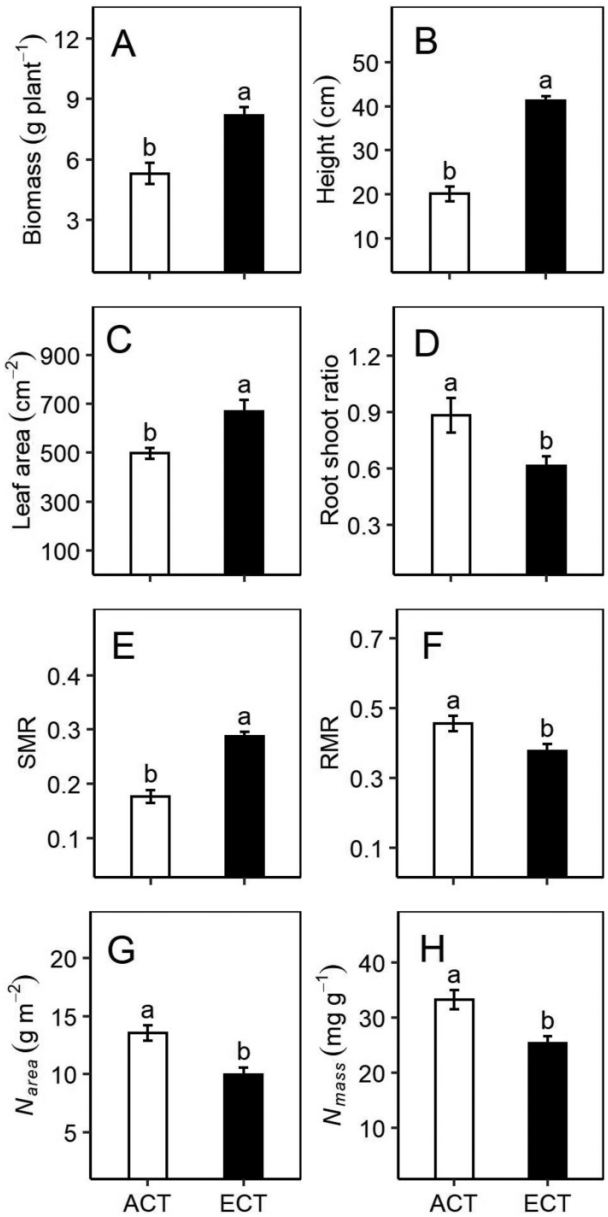

Table 3. Effects of CO_2–temperature treatment (mean ± SE, $n = 6$) on photosynthetic variables of white birch.

Photosynthetic variable	ACT	ECT
V_{cmax} (μmol·m^{-2}·s^{-1})	75.8 ± 2	49 ± 2.2
J_{max} (μmol·m^{-2}·s^{-1})	262 ± 10.4	122.7 ± 6.3
J_{max}/V_{cmax}	3.5 ± 0.17	2.6 ± 0.05
J_{max}/N_{area} (μmol·g^{-2}·s^{-1})	19.8 ± 1.8	12.7 ± 1.3
R_d (μmol·m^{-2}·s^{-1})	1.53 ± 0.13	0.76 ± 0.06
R_l (μmol·m^{-2}·s^{-1})	3.2 ± 0.21	1.1 ± 0.11
g_m (mol·m^{-2}·s^{-1})	0.25 ± 0.008	0.12 ± 0.004
C_i* (μmol·mol^{-1})	38.6 ± 2.65	45.9 ± 1.02
ΦPHII	0.37 ± 0.02	0.18 ± 0.01
J_c (μmol·m^{-2}·s^{-1})	101.8 ± 3.5	59.6 ± 2.3
J_o (μmol·m^{-2}·s^{-1})	24.2 ± 2.5	6.6 ± 1.1
J_c/J_o	4.4 ± 0.5	8.8 ± 1.0

Note: The seedlings were grown either under ACT (ambient 400 μmol·mol^{-1} CO_2 and ambient temperature) or ECT (750 μmol·mol^{-1} CO_2 and elevated temperature (ambient + 4 °C)). The treatment effects were all statistically significant ($P \leq 0.05$). See Tables 1 and 2 for other explanations.

Fig. 2. PCA (using FactoMineR package in R) of growth and photosynthetic parameters with significant treatment effects (ACT vs. ECT). The polygons indicate treatment clustering. The biaxial diagrams were generated by the factoextra package in R. Abbreviations: C_i*, intercellular CO_2 compensation point; CCP_{aci}, C_i compensation point from A/C_i curve; J_c/J_o, ratio of electron transport of carboxylation (J_c) to oxygenation (J_o) ; J_{max}/N_{area}, max electron transport rate per unit leaf N; V_{cmax}, maximum rate of ribulose-1,5-bisphosphate carboxylation; J_{max}, maximum of photosynthetic electron transport rate; A_{n-t}, net photosynthesis rate at the transition point between rubisco limitation and RuBP regeneration limitation based on A/C_i curve; ΦPHII, photochemical efficiency of photosystem II; g_m, mesophyll conductance; N_{mass}, leaf N concentration based mass; R_d, daytime respiration; and N_{area}, leaf N per unit area in white birch seedlings. See Fig. 1 for other explanations.

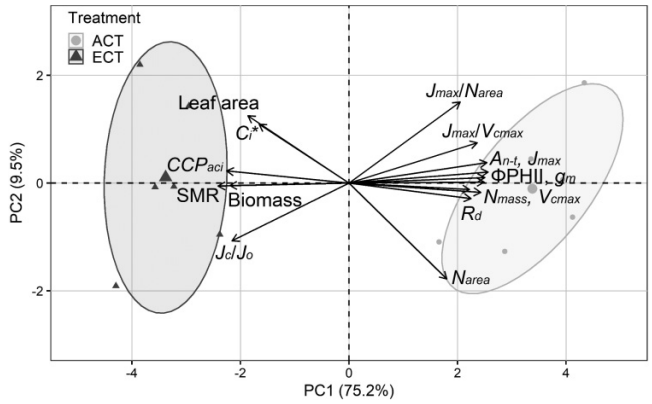

rameters (i.e., V_{cmax}, J_{max}, ACE, and ΦPHII), positively correlated with growth parameters, particularly height growth, but had no significant relationship with leaf area (Table 4). Total leaf area per tree was negatively correlated to N_{mass}, N_{area}, and RMR (Figs. 3A, 3B, and 3D), and positively related to SMR (Fig. 3E). Interestingly, there was no significant correlation between leaf area and SLA and LMR (Figs. 3C and 3F).

Table 4. Pearson correlation coefficients between CCP_{aci} and photosynthetic/growth variables and between and J_c/J_o and photosynthetic/growth variables in birch seedlings.

Variable	CCP_{aci}	J_c/J_o
V_{cmax}	−0.83**	−0.79**
J_{max}	−0.84**	−0.84**
ACE	−0.83**	−0.82**
ΦPHII	−0.86**	−0.76**
Biomass	0.75*	0.85**
Height	0.75*	0.64*
SMR	0.69*	0.7*
Leaf area	0.6*	0.29

Note: CCP_{aci}, CO_2 compensation point from A/C_i curve; J_c/J_o, ratio of electron transport to carboxylation (J_c) and to oxygenation (J_o); V_{cmax}, maximum rate of ribulose-1,5-bisphosphate carboxylation; J_{max}, maximum of photosynthetic electron transport rate; ACE, apparent carboxylation efficiency; ΦPHII, photochemical efficiency of photosystem II. *, $0.01 < P \leq 0.05$; **, $P \leq 0.01$.

Table 5. P values of two-way ANOVA for the effects of measurement C_a, CO_2–temperature treatment, and their interactions on A_n, g_s, E, C_i/C_a, and iWUE.

Variable	C_a	Treatment	C_a × Treatment
A_n	<0.001	<0.001	**0.034**
g_s	0.791	**<0.001**	0.478
C_i/C_a	**0.04**	0.558	0.949
iWUE	**<0.001**	**<0.001**	0.058

Note: Seedlings were grown under ACT or ECT and measured at 400 and 750 μmol·mol^{-1} CO_2 (C_a). Significant effects ($P \leq 0.05$) are in bold. A_n, net photosynthesis rate; C_i/C_a, intercellular (C_i) to ambient (C_a) CO_2 concentration ratio; g_s, stomatal conductance; iWUE, instantaneous photosynthetic water use efficiency.

A/C_i curve transition point, CO_2 compensation point and respiration

ECT substantially lowered the A/C_i curves (Fig. 4), indicating photosynthetic downregulation. However, ECT did not significantly affect the C_i transition point (C_{i-t}, A_{n-t}) of photosynthetic limitation by carboxylation restriction and by RuBP regeneration restriction although it significantly reduced A_{n-t} (Figs. 4A and 4B). A_{n-t} was positively correlated with photosynthetic capacity variables, but negatively correlated with biomass, SMR, J_c/J_o, and CCP_{aci}. ECT increased CCP_{aci} but decreased ACE (Figs. 4A and 4B). It is interesting to note that ECT significantly increased the CO_2 compensation point directly derived from the A/C_i curve (CCP_{aci}) but had no significant effect on the CO_2 compensation point derived using the Laisk method (C_i*, in Table 2).

Interactions between measurement CO_2 concentration and CO_2–temperature treatment

The 400 μmol·mol^{-1} measurement CO_2 resulted in significant lower A_n, iWUE, and lower C_i/C_a (Figs. 5A, 5C, and 5D), but the effect on A_n was greater under ECT than under ACT (63.9% vs. 53%) (Table 5; Fig. 5A). ECT significantly reduced A_n measured at the same CO2 concentration (both 400 and 750 μmol·mol^{-1}; Fig. 5A) as well as g_s and iWUE measured at the corresponding growth C_a (Figs. 5B and 5C).

Discussion

Photosynthetic acclimation and optimal carbon gain theory

Elevated CO_2 often leads to photosynthetic acclimation, which is manifested as declines in photosynthetic capacity, respiratory rate, stomatal conductance, and leaf nitrogen concentration (Kizildeniz et al. 2021; Yin et al. 2019). Acclimation is defined as the morphological and (or) physiological adjustments of a plant to compensate for alterations in performance caused by environmental changes (Bermudez et al. 2021). Both elevations in CO_2 and higher temperature can lead to acclimation (Murphy and Way 2021). It is generally believed that photosynthetic acclimation is mainly caused by elevated CO_2 and has no direct relationship with temperature and water conditions (Salazar-Parra et al. 2015). Elevated CO_2 increases the substrate for photosynthesis, alleviates the carboxylation limit of RuBP, leads to decreases in V_{cmax} and g_s (Dusenge et al. 2019), and reduces respiration (Birami et al. 2020). Although photosynthetic acclimation can vary between species, acclimation generally leads to the maximization carbon sequestration (Smith and Dukes 2017).

Increasing temperature can lead to thermal acclimation, such as accelerating processes related to leaf carbon flux, including photosynthesis and respiration, thus driving an increase in carbon sink intensity (Smith and Dukes 2017; Weigt et al. 2018). Warming stimulates the activation of photosynthetic enzymes such as rubisco and reduces the sensitivity of photorespiration to temperature (Cai et al. 2018). Due to the different effects of photosynthetic acclimation to CO_2 and thermal acclimation, it is difficult to predict plant responses under elevated CO_2 and warmer temperature in future environmental conditions (Bermudez et al. 2021). Some studies believe that combined effects of elevated CO_2 and warmer temperature are positive to plants by promoting plant growth and enhancing stress resistance (Apgaua et al. 2019). Other studies, however, find that the effects of the two factors offset each other and the combination has no net effects on plants (Dusenge et al. 2019). Our results show that white birch seedlings in the ECT treatment exhibited typical photosynthetic acclimation. The 4 °C increase in temperature did not change the pattern of photosynthetic acclimation, such as the reductions in photosynthetic capacity and respiration.

Electron flow partitioning and limitations of photosynthesis

Photosynthetic acclimation is a part of the process to optimize the operation of photosynthesis when the environmental conditions change (Yin et al. 2019). The causes of photosynthetic acclimation include the inhibition of nitrogen assimilation and photorespiration and the negative feedback of rubisco and electron transport constraints on photosynthesis (Dusenge et al. 2019). One theory is that the increase in growth resulting from increases in carbohydrate production and limited nutrient supply lead to the dilution of N in leaves, and consequently reduce the amount of

Fig. 3. Relationships between leaf area and leaf-mass based N concentration (A); leaf area-based N (B); SLA (C); RMR (D); SMR (E); and LMR (F) in birch seedlings. The seedings were grown either under ACT (triangles) or ECT (diamond). See Fig. 1 for other explanations.

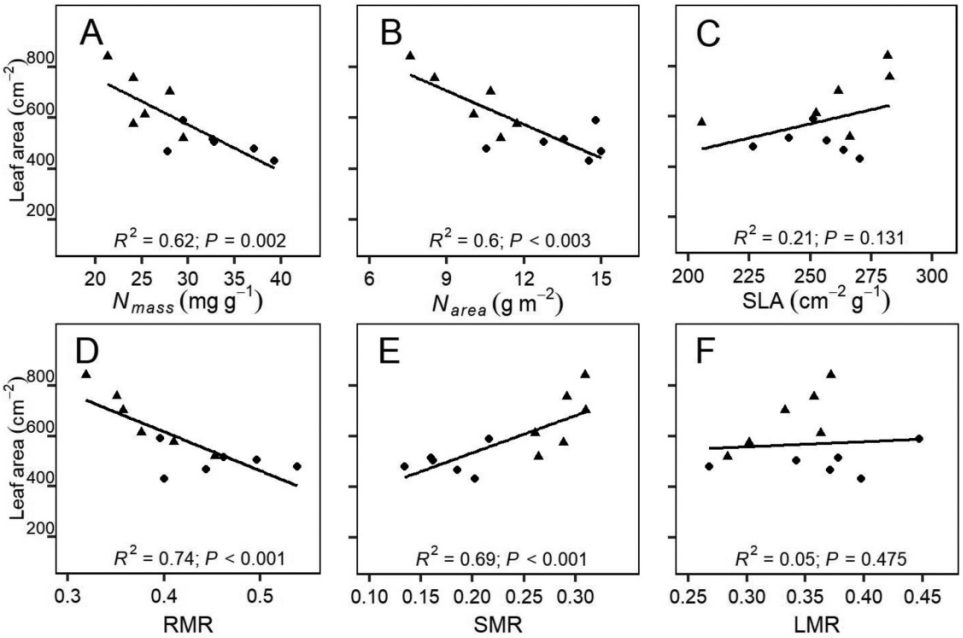

Fig. 4. A/C_i curves of birch seedlings grown either under ACT (A) and ECT (B). Each point in the plots represents the average of six sample trees. The open circle at the crossing point in each plot denotes the transition point (C_{i-t}, A_{n-t}) from rubisco limitation to RuBP limitation. The analysis was conducted using the "findCiTransition" function in the R "plantecophys" package. ACE: apparent carboxylation efficiency derived from the initial slope of the A/C_i curve; CCP_{aci}: CO_2 compensation point derived from A/C_i curve, i.e., C_i when A_n was zero. Both ACE and CCP_{aci} were significantly different between ACT and ECT ($P \leq 0.05$).

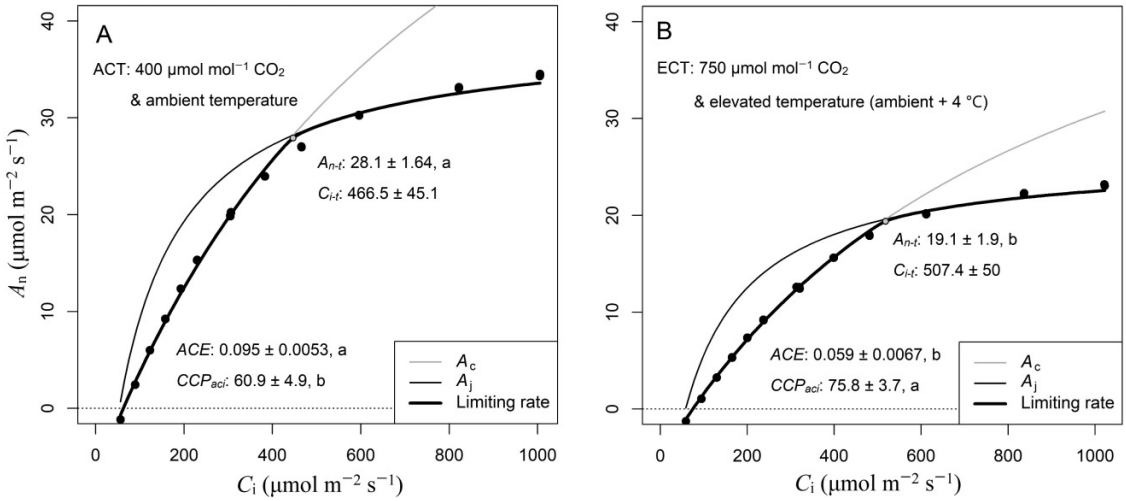

photosynthetic machinery (Byeon et al. 2021). It is believed that photosynthetic acclimation serves to optimize resource allocation and maximize growth under limited resources (Slot and Winter 2017; Smith et al. 2019). We found that ECT caused significant decreases in J_c and J_o, but a significant increase in J_c/J_o ratio, indicating that the proportion of electrons partitioned to carboxylation increased although the photosynthetic capacity per unit leaf decreased. Some studies have shown that J_c is the cause of the decline of photosynthesis under elevated CO_2 (Smith and Keenan 2020), suggesting that J_c may play a key role in the photosynthetic acclimation of white birch.

The elevated CO_2 and higher temperature shifted the limitation of photosynthesis from RuBP carboxylation limitation to RuBP regeneration limitation in white birch, which is consistent with the literature (Kumarathunge et al. 2019; Suzuki et al. 2021). However, at the point of co-limitation by carboxylation and RuBP regeneration, A_{n-t}, the photosynthetic rate at the transition point can comprehensively reflect the effects

Fig. 5. Effects of CO_2–temperature combination treatment (ACT vs. ECT), measurement CO_2 concentration (C400: 400 μmol·mol^{-1} C_a *vs.* C750: 750 μmol·mol^{-1} C_a), and their interactions on A_n (A), g_s (B), iWUE (C), C_i/C_a (D). Means (±1.96 × SE, $n = 6$) with different letters are significantly different from each other ($P \leq 0.05$). ACT-C400 and ACT-C750 represent the photosynthetic rates of seedlings grown under ACT but measured at 400 and 750 μmol·mol^{-1} CO_2, respectively, while ECT-C400 and ECT-C750 were the photosynthetic rates of seedlings grown under ECT but measured at 400 and 750 μmol·mol^{-1} C_a, respectively. See Table 1 for other explanations.

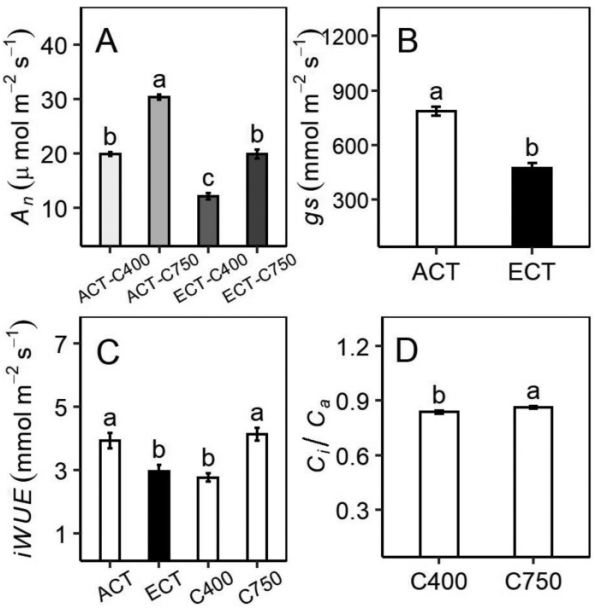

of V_{cmax}, J_{max}, g_s, and C_i on the photosynthetic rate (Taylor et al. 2020). Our data show that the C_{i-t} was greater than the corresponding C_i under ECT treatment, indicating that photosynthesis was primarily limited by RuBP regeneration. Furthermore, our data suggests that acclimation to the higher temperature in ECT was primarily responsible for the shift of mechanisms of photosynthetic limitation in white birch rather than acclimation the elevated CO_2. Elevated CO_2 generally increases the J_{max}/V_{cmax} ratio (Ainsworth and Rogers 2007 ; Smith and Keenan 2020). In contrast, warmer temperatures tend to decrease the J_{max}/V_{cmax} ratio (Kumarathunge et al. 2019; Bermudez et al. 2021). The ECT treatment in this study significantly reduced the J_{max}/V_{cmax} ratio, indicating that the warmer temperature in the ECT treatment had a greater impact than the elevated CO_2 on the nitrogen partitioning between the machinery for electron transport related to RuBP regeneration (J_{max}) and that for CO_2 reduction (V_{cmax}) in white birch, as reported for some other plant species (Kumarathunge et al. 2019).

Total versus per-unit leaf area based photosynthetic parameters

It is not uncommon that leaf-area based photosynthetic variables show opposite responses to elevated CO_2 than biomass and growth (Kanno et al. 2017). The opposite response trends are related to the assessment of responses at different levels, i.e., per unit leaf area versus the whole plant (Xu et al. 2021), and can be explained by the differences in total leaf area per tree. This study found that the ECT significantly reduced the values of some key leaf-area based parameters related to photosynthetic capacity (i.e., down regulation), such as V_{cmax} and J_{max}, but increased seedling biomass in white birch. However, the photosynthetic rate measured at the corresponding growth CO_2 concentration (A400 for ACT and E750 for ECT in Fig. 5A) was not significantly different between the two treatments. While the similar photosynthetic rates and differences in biomass appear to contradict each other, the difference can be explained by differences in the total leaf area per tree. These responses can be attributed the combined effect of higher temperature and elevated CO_2 in the ECT treatment (Dusenge et al. 2019). These results indicate that the photosynthetic machinery of white birch was downregulated in response to the ECT treatment, but the entire photosynthetic system acclimated to the treatment CO_2 and temperature such that the actual operational rate of photosynthesis remained about the same between the two treatments. Furthermore, our data show that the greater rates of growth and carbon sequestration in the ECT treatment were primarily driven by the greater amount of leaf area per tree in the trees grown under ECT. This conclusion is consistent with the findings of some other studies (Wang et al. 2020). Furthermore, the increased production of new leaves can serve as temporary sinks and reduce the feedback inhibition to photosynthesis by the accumulation of excess photosynthates under elevated CO_2 (Beechey-Gradwell et al. 2020; Smith and Keenan 2020). Some studies suggest that carbon sink intensity is mainly driven by elevated temperature, rather than the result of increased carbon assimilation under elevated CO_2 (Weigt et al. 2018).

CO_2 compensation point and respiration

CO_2 and temperature can cause metabolic reorganization in plants (Tausz-Posch et al. 2020). Elevated CO_2 can inhibit plant respiration, R_d or R_l or both, indicating less energy consumption (Jauregui et al. 2015), but higher temperatures tend to increase respiration and decrease the temperature sensitivity of photorespiration (Cai et al. 2018). Interestingly, the ECT treatment in this study significantly increased the CO_2 compensation point (both C_i* and CCP_{aci}) and CCP_{aci} was closely correlated with biomass variables. The CO_2 compensation point reflects the photorespiratory loss of CO_2 and the kinetic properties of rubisco (Walker and Cousins 2013), and the CCP_{aci} reflects the effects of the total respiration, including both R_l and R_d which depends on reductants generated by photosynthetic electron transfer (Wujeska-Klause et al. 2019; Tcherkez and Atkin 2021). The results showed that ECT treatment significantly increased CCP_{aci} of white birch. We speculated that CCP_{aci} might be related to the decrease of rubisco carboxylation ability because photorespiration did not decrease but decreased. Meanwhile, the negative correlation between CCP_{aci} and photosynthesis ability also supported this result. Warming usually causes an increase in

photorespiration (Dusenge et al. 2020), but we observed the opposite result, suggesting that the increase of CCP_{aci} in white birch photosynthetic acclimation may not be directly related to the increase in ambient temperature. The positive relationship between CCP_{aci} and biomass could be suggested that the CO_2 compensation point may reflect some comprehensive effect of photosynthetic acclimation and may also be affected by temperature increase. However, the potential mechanism needs to be further studied.

Conclusions

White birch exhibited typical photosynthetic acclimations to the elevation of CO_2 and warming at the leaf level, such as reductions in V_{cmax}, J_{max}, A_n, R_l, R_d, N_{mass}, g_s, and g_m. The increase in total leaf area, however, more than offset the negative effect of the leaf-level photosynthetic downregulation on the total carbon assimilation of the tree. Furthermore, the increase in electron partitioning to carboxylation, as indicated by an increase in J_c/J_o and decreases in respiration (both R_l and J_o) may play a critical role in the acclimation of white birch to the elevation of CO_2 and warmer temperature. The 4 °C increase in temperature did not change the pattern of photosynthetic acclimation. However, warming may have played a key role in the decrease of J_{max}/V_{cmax} ratio in the seedlings subjected to ECT, which contributed to the photosynthetic downregulation. Overall, the responses of white birch to elevated CO_2 and higher temperature are consistent with the optimal carbon gain theory, and carbon gain drove the coordination between carboxylation, electron transfer, stomatal regulation, and respiration to maximize carbon assimilation. This study was conducted using pots and under controlled environment in the greenhouse. Pot limitations can lead to an underestimation of treatment effects because the limitation will be more severe to larger plants in the treatment that promotes photosynthesis and (or) growth. However, Binyam et al. (Binyam et al. 2021) find that pot limitation does not occur in white birch under a treatment similar to that of the current study.

Acknowledgements

We want to thank Ms. Keri Pidgen, the greenhouse manager, for her logistic support and other operational assistance during the experiments. The study was supported by an NSERC Discovery Development Grant to QLD (Project No. DDG-2020–00008).

Article information

History dates

Received: 21 March 2022
Accepted: 14 June 2022
Accepted manuscript online: 20 June 2022
Version of record online: 19 August 2022

Copyright

Data availability

Data available upon request.

Author information

Author ORCIDs

Qing-Lai Dang https://orcid.org/0000-0002-5930-248X

Competing interests

The authors declare there are no competing interests.

References

Ainsworth, E.A., and Long, S.P. 2021. 30 years of free-air carbon dioxide enrichment (FACE): what have we learned about future crop productivity and its potential for adaptation? Global Change Biol. **27**(1): 27–49. doi: 10.1111/gcb.15375.

Ainsworth, E.A., and Rogers, A. 2007. The response of photosynthesis and stomatal conductance to rising [CO2]: mechanisms and environmental interactions. Plant Cell Environ. **30**(3): 258–270.

Apgaua, D.M.G., Tng, D.Y.P., Forbes, S.J., Ishida, Y.F., Vogado, N.O., Cernusak, L.A., and Laurance, S.G.W. 2019. Elevated temperature and CO_2 cause differential growth stimulation and drought survival responses in eucalypt species from contrasting habitats. Tree Physiol. **39**(11): 1806–1820. doi: 10.1093/treephys/tpz095. PMID: 31768554.

Beechey-Gradwell, Z., Cooney, L., Winichayakul, S., Andrews, M., Hea, S.Y., Crowther, T., and Roberts, N. 2020. Storing carbon in leaf lipid sinks enhances perennial ryegrass carbon capture especially under high N and elevated CO_2. J. Exp. Bot. **71**(7): 2351–2361. doi: 10.1093/jxb/erz494. PMID: 31679036.

Bermudez, R., Stefanski, A., Montgomery, R.A., and Reich, P.B. 2021. Short- and long-term responses of photosynthetic capacity to temperature in four boreal tree species in a free-air warming and rainfall manipulation experiment. Tree Physiol. **41**(1): 89–102. doi: 10.1093/treephys/tpaa115. PMID: 32864704.

Binyam, T., Qing-Lai, D., and Sahari, I. 2021. Longer photoperiods negate the CO_2 stimulation of photosynthesis in *B etula papyrifera* Marshall: implications to climate change-induced migration. Physiol. Plant. **172**(1): 106–115. PMID: 33280131.

Birami, B., Nägele, T., Gattmann, M., Preisler, Y., Gast, A., Arneth, A., and Ruehr, N.K. 2020. Hot drought reduces the effects of elevated CO2 on tree water-use efficiency and carbon metabolism. New Phytol. **226**(6): 1607–1621. doi: 10.1111/nph.16471. PMID: 32017113.

Byeon, S., Song, W., Park, M., Kim, S., Kim, S. Lee, H., et al. 2021. Downregulation of photosynthesis and its relationship with changes in leaf N allocation and N availability after long-term exposure to elevated CO_2 concentration. J. Plant Physiol. **265**: 153489. doi: 10.1016/j.jplph.2021.153489. PMID: 34416600.

Cai, C., Li, G., Yang, H., Yang, J., Liu, H. Struik, P.C., et al. 2018. Do all leaf photosynthesis parameters of rice acclimate to elevated CO2, elevated temperature, and their combination, in FACE environments? Global Change Biol. **24**(4): 1685–1707. doi: 10.1111/gcb.13961.

Dingkuhn, M., Luquet, D., Fabre, D., Muller, B., Yin, X., and Paul, M.J. 2020. The case for improving crop carbon sink strength or plasticity for a CO_2-rich future. Curr. Opin. Plant Biol. **56**: 259–272. doi: 10.1016/j.pbi.2020.05.012. PMID: 32682621.

Dusenge, M.E., Duarte, A.G., and Way, D.A. 2019. Plant carbon metabolism and climate change: elevated CO_2 and temperature impacts on photosynthesis, photorespiration, and respiration. New Phytol. **221**(1): 32–49. doi: 10.1111/nph.15283. PMID: 29983005.

Dusenge, M.E., Madhavji, S., and Way, D.A. 2020. Contrasting acclimation responses to elevated CO 2 and warming between an evergreen and a deciduous boreal conifer. Global Change Biol. **26**(6): 3639–3657. doi: 10.1111/gcb.15084.

Duursma, R.A. 2015. Plantecophys—An r package for analysing and modelling leaf gas exchange data. PLoS ONE, **10**(11): e0143346. doi: 10.1371/journal.pone.0143346. PMID: 26581080.

Farquhar, G.D., von Caemmerer, S., and Berry, J.A. 1980. A biochemical model of photosynthetic CO_2 assimilation in leaves of C3 species [online]. Planta, **149**: 78–90. doi: 10.1007/BF00386231. PMID: 24306196.

Harley, P.C., Loreto, F., Marco, G.D., and Sharkey, T.D. 1992. Theoretical considerations when estimating the mesophyll conductance to CO_2 flux analysis of the response of photosysthesis to CO_2 [online]. Plant Physiol. **98**: 1429–1436. doi: 10.1104/pp.98.4.1429. PMID: 16668811.

Jauregui, I., Aroca, R., Garnica, M., Zamarreño, Á.M., García-Mina, J.M. Serret, M.D., et al. 2015. Nitrogen assimilation and transpiration: key processes conditioning responsiveness of wheat to elevated CO_2 and temperature. Physiol. Plant. **155**(3): 338–354. doi: 10.1111/ppl.12345. PMID: 25958969.

Jayawardena, D.M., Heckathorn, S.H., Bista, D.R., and Boldt, J.K. 2019. Elevated carbon dioxide plus chronic warming causes dramatic increases in leaf angle in tomato, which correlates with reduced plant growth. Plant Cell Environ. **42**(4): 1247–1256.

Kanno, K., Suzuki, Y., and Makino, A. 2017. A small decrease inrubisco content by individual suppression of RBCS genes leads to improvement of photosynthesis and greater biomass production in rice under conditions of elevated CO_2. Plant Cell Physiol. **58**(3): 635–642. doi: 10.1093/pcp/pcx018. PMID: 28158810.

Kimball, B.A. 2016. Crop responses to elevated CO_2 and interactions with H2O, N, and temperature. Curr. Opin. Plant Biol. **31**: 36–43. doi: 10.1016/j.pbi.2016.03.006. PMID: 27043481.

Kizildeniz, T., Pascual, I., Irigoyen, J.J., and Morales, F. 2021. Future CO_2, warming and water deficit impact white and red Tempranillo grapevine: photosynthetic acclimation to elevated CO_2 and biomass allocation. Physiol. Plant. **172**(3): 1779–1794. doi: 10.1111/ppl.13388. PMID: 33704796.

Kumarathunge, D.P., Medlyn, B.E., Drake, J.E., Rogers, A., and Tjoelker, M.G. 2019. No evidence for triose phosphate limitation of light-saturated leaf photosynthesis under current atmospheric CO_2 concentration. Plant Cell Environ. **42**(12): 3241–3252.

Kurepin, L.V., Stangl, Z.R., Ivanov, A.G., Bui, V., Mema, M. Hüner, N.P.A., et al. 2018. Contrasting acclimation abilities of two dominant boreal conifers to elevated CO_2 and temperature. Plant Cell Environ. **41**(6): 1331–1345.

Momayyezi, M., and Guy, R.D. 2017. Substantial role for carbonic anhydrase in latitudinal variation in mesophyll conductance of *P opulus trichocarpa* Torr. & Gray. Plant Cell Environ. **40**(1): 138–149.

Murphy, B.K., and Way, D.A. 2021. Warming and elevated CO_2 alter tamarack C fluxes, growth and mortality: evidence for heat stress-related C starvation in the absence of water stress. Tree Physiol. **41**(12): 2341–2358. doi: 10.1093/treephys/tpab077. PMID: 34077546.

Pastore, M.A., Lee, T.D., Hobbie, S.E., and Reich, P.B. 2019. Strong photosynthetic acclimation and enhanced water-use efficiency in grassland functional groups persist over 21 years of CO_2 enrichment, independent of nitrogen supply. Global Change Biol. **25**(9): 3031–3044. doi: 10.1111/gcb.14714.

Potvin, C., and Tardif, S. 1988. Sources of variability and experimentaldesigns in growth chambers. Funct. Ecol. **2**: 123–130. doi:10.2307/2389472

Salazar-Parra, C., Aranjuelo, I., Pascual, I., Erice, G., Sanz-Sáez, A. Aguirreolea, J., et al. 2015. Carbon balance, partitioning and photosynthetic acclimation in fruit-bearing grapevine (*Vitis vinifera* L. cv. Tempranillo) grown under simulated climate change (elevated CO_2, elevated temperature, and moderate drought) scenarios in temperature gradient greenhouses. J. Plant Physiol. **174**: 97–109. PMID: 25462972.

Slot, M., and Winter, K. 2017. Photosynthetic acclimation to warming in tropical forest tree seedlings. J. Exp. Bot. **68**(9): 2275–2284. doi: 10.1093/jxb/erx071. PMID: 28453647.

Slot, M., Rifai, S.W., and Winter, K. 2021. Photosynthetic plasticity of a tropical tree species, *T abebuia rosea*, in response to elevated temperature and CO_2. Plant Cell Environ. **44**(7): 2347–2364.

Smith, N.G., and Dukes, J.S. 2017. Short-term acclimation to warmer temperatures accelerates leaf carbon exchange processes across plant types. Global Change Biol. **23**(11): 4840–4853. doi: 10.1111/gcb.13735.

Smith, N.G., and Keenan, T.F. 2020. Mechanisms underlying leaf photosynthetic acclimation to warming and elevated CO_2 as inferred from least-cost optimality theory. Global Change Biol. **26**(9): 5202–5216. doi: 10.1111/gcb.15212.

Smith, N.G., Keenan, T.F.,Prentice, I.C.,Wang, H., Wright, I.J., Niinemets, U., et al. 2019. Global photosynthetic capacity is optimized to the environment. Ecol. Lett. **22**(3): 506–517. doi: 10.1111/ele.13210. PMID: 30609108.

Suzuki, Y., Ishiyama, K., Sugawara, M., Suzuki, Y., Kondo, E. Takegahara-Tamakawa, Y., et al. 2021. Overproduction of chloroplast glyceraldehyde-3-phosphate dehydrogenase improves photosynthesis slightly under elevated CO_2 conditions in rice. Plant Cell Physiol. **62**(1): 156–165. doi: 10.1093/pcp/pcaa149. PMID: 33289530.

Tausz-Posch, S., Tausz, M., and Bourgault, M. 2020. Elevated CO2 effects on crops: advances in understanding acclimation, nitrogen dynamics and interactions with drought and other organisms. Plant Biol. **22**(Suppl 1): 38–51. doi: 10.1111/plb.12994. PMID: 30945436.

Taylor, S.H., Orr, D.J., Carmo-Silva, E., and Long, S.P. 2020. During photosynthetic induction, biochemical and stomatal limitations differ between *Brassica* crops. Plant Cell Environ. **43**(11): 2623–2636.

Tcherkez, G., and Atkin, O.K. 2021. Unravelling mechanisms and impacts of day respiration in plant leaves: an introduction to a Virtual Issue. New Phytol. **230**: 5–10. doi:10.1111/nph.17164

Tcherkez, G., Gauthier, P., Buckley, T.N., Busch, F.A., Barbour, M.M. Bruhn, D., et al. 2017. Leaf day respiration: low CO_2 flux but high significance for metabolism and carbon balance. The New Phytologist, **216**(4): 986–1001. doi: 10.1111/nph.14816. PMID: 28967668.

Tomeo, N.J., and Rosenthal, D.M. 2018. Photorespiration differs among *A rabidopsis thaliana* ecotypes and is correlated with photosynthesis. J. Exp. Bot. **69**(21): 5191–5204. doi: 10.1093/jxb/ery274. PMID: 30053111.

Valentini, R., Epron, D., Angelis, P.D., Matteucci, G., and Dreyer, E. 1995. In situ estimation of net CO_2 assimilation, photosynthetic electron flow and photorespiration in Turkey oak (*Q. cerris* L.) leaves: diurnal cycles under different levels of water supply [online]. Plant Cell Environ. **18**: 631–640. doi: 10.1111/j.1365-3040.1995.tb00564.x.

Walker, B.J., and Cousins, A.B. 2013. Influence of temperature on measurements of the CO_2 compensation point: differences between the Laisk and O_2-exchange methods. J. Exp. Bot. **64**(7): 1893–1905. doi: 10.1093/jxb/ert058. PMID: 23630324.

Wang, F., Gao, J., Yong, J.W.H., Wang, Q., Ma, J., and He, X. 2020. Higher atmospheric CO_2 levels favor C3 plants over C4 plants in utilizing ammonium as a nitrogen source. Front. Plant Sci. **11**: 537443. doi: 10.3389/fpls.2020.537443. PMID: 33343587.

Weigt, R.B., Streit, K., Saurer, M., and Siegwolf, R.T. 2018. The influence of increasing temperature and CO_2 concentration on recent growth of old-growth larch: contrasting responses at leaf and stem processes derived from tree-ring width and stable isotopes. Tree Physiol. **38**(5): 706–720. doi: 10.1093/treephys/tpx148.

Wujeska-Klause, A., Crous, K.Y., Ghannoum, O., and Ellsworth, D.S. 2019. Lower photorespiration in elevated CO_2 reduces leaf N concentrations in mature eucalyptus trees in the field. Global Change Biol. **25**(4): 1282–1295. doi: 10.1111/gcb.14555.

Xu, H., Wang, H., Prentice, I.C., Harrison, S.P., Wang, G., and Sun, X. 2021. Predictability of leaf traits with climate and elevation: a case study in Gongga Mountain, China. Tree Physiol. **41**(8): 1336–1352. doi: 10.1093/treephys/tpab003. PMID: 33440428.

Yin, X., Schapendonk, A.H.C.M., and Struik, P.C. 2019. Exploring the optimum nitrogen partitioning to predict the acclimation of C_3 leaf photosynthesis to varying growth conditions. J. Exp. Bot. **70**(9): 2435–2447. doi: 10.1093/jxb/ery277. PMID: 30053195.